Asymmetric Electrochemical Polymerization: Preparation of Polybithiophene in a Chiral Nematic Liquid Crystal Field and Optically Active Electrochromism

Hiromasa Goto and Kazuo Akagi*

Tsukuba Research Center for Interdisciplinary Materials Science (TIMS), Institute of Materials Science, University of Tsukuba, Tsukuba, Ibaraki 305-8573, Japan

Received July 21, 2004; Revised Manuscript Received October 15, 2004

ABSTRACT: Optically active polybithiophene is successfully prepared by electrochemical polymerization in a chiral nematic liquid crystal field. Polarizing and phase-contrast optical micrographs of the polymer reveal a well-resolved spiral morphology similar to the optical texture of the chiral nematic phase. Circular dichroism measurements indicate the Cotton effect for the film. The polymer exhibits optically active electrochromism and switching behavior. Synthesis in a thermotropic chiral liquid crystal field therefore represents a new technique for the preparation of chiral conducting polymer films.

Introduction

There have been a great number of studies on optically active polymers in relation to the synthesis of polypeptides, vinyl polymers, and helical conjugated polymers. Optically active polymers have been obtained by several methods, including the polymerization of optically active monomers,[1−7] asymmetric selective polymerization,[8,9] and introduction of an chiral group into an optically inactive polymer by polymer reactions.[10] The polymers prepared by such methods contain an asymmetric carbon in the side chain or in the main chain. Although it is also possible to synthesize a conjugated polymer with one screw sense through the use of an optically active catalyst, the chirality of such polymers, without a bulky substituent, will be lost upon melting and dissolution. Helical polyacetylene with chiroptical properties has been synthesized in chiral nematic liquid crystal as a reaction field.[11,12] The helical polyacetylene prepared in this way exhibits relatively stable chirality as a result of its insolubility and infusibility. Scanning electron microscopy (SEM) of the helical polyacetylene surface has revealed that the polymer forms a clear helical morphology with hierarchy, strongly suggesting that the chirality of the helical polyacetylene originates from the one-handed helical form of the polymer main chain.

Chemical synthesis of a polymer such as polyacetylene requires careful treatment using a highly air-sensitive catalytic system composed of *tetra-n*-butoxytitanium/triethylaluminum. In contrast, the equivalent electrochemical synthesis is simple and safe for the preparation of conjugated polymers. Electrochemical polymerization can be used to produce many kinds of conjugated polymers, such as polypyrrole, polythiophene, poly(3,4-ethylenedioxythiophene) (PEDOT), and poly(3,4-ethylenedioxypyrrole) (PEDOP).[13] These polymers have been investigated for potential application in electrochromic devices,[14] as the buffer layer of electroluminescent devices,[15,16] and in sensors.[17] However, the polymer films synthesized by electrochemical polymerization usually exhibit neither linear nor circular dichroism. In our previous work, a new electrochemical polymerization method employing a chiral nematic liquid crystal (N*-LC) field was developed for the preparation of nonsubstituted optically active PEDOT (PEDOT*) with chirality.[18] In this research, the electrochemical polymerization of bithiophene was performed using N*-LC as an asymmetric and anisotropic reaction field for the preparation of optically active polybithiophene (PBTh*) without chiral and bulky substituents in the polymer. The Cotton effect of PBTh* prepared in the N*-LC field was stronger than that of PEDOT*, attributable to the stronger affinity of the bithiophene monomer to the N*-LC field (due to linearity and molecular shape) and the resultant enhancement of field replication during polymerization.

* Corresponding author. E-mail: akagi@ims.tsukuba.ac.jp.

Preparation of Chiral Nematic Electrolyte

The addition of a small amount of an optically active molecule as a chiral dopant to a nematic liquid crystal (N-LC) can induce the formation of chiral N-LC (N*-LC) with helical structures on a mesoscopic level.[19,20] The director of N*-LC rotates gradually in one screw direction to form a helical structure. The liquid crystallinity of 4-cyano-4′-*n*-hexyl biphenyl (6CB) has been confirmed to be maintained after the addition of tetrabutylammonium perchlorate (TBAP) as a supporting salt and bithiophene as a monomer, and the addition of a small amount of chiral dopant has been found to induce chiral nematic liquid crystallinity in the mixed system. Although the chiral dopant itself exhibits no liquid crystallinity, it induces a chiral nematic phase. The material 6CB with thermotropic LC can be regarded as a solvent of fluidity, and the addition of a supporting salt to 6CB provides ionic conductivity. Therefore, a mixture of LC and a supporting salt can be used as an electrolyte for electrochemical polymerization instead of normal systems such as TBAP or lithium perchlorate in acetonitrile.

In the present synthesis, 6CB was adopted as the solvent for asymmetric electrochemical polymerization. The molecular structures of the materials used are shown in Scheme 1.

A N*-LC mixture consisting of 42 mM of (*R*)- or (*S*)-PCH506-Binol (chiral dopant), 0.48 M of bithiophene (monomer), and 3 mM of TBAP (supporting salt) in 6CB

10.1021/ma048505n CCC: $30.25
Published on Web 01/25/2005

Scheme 1

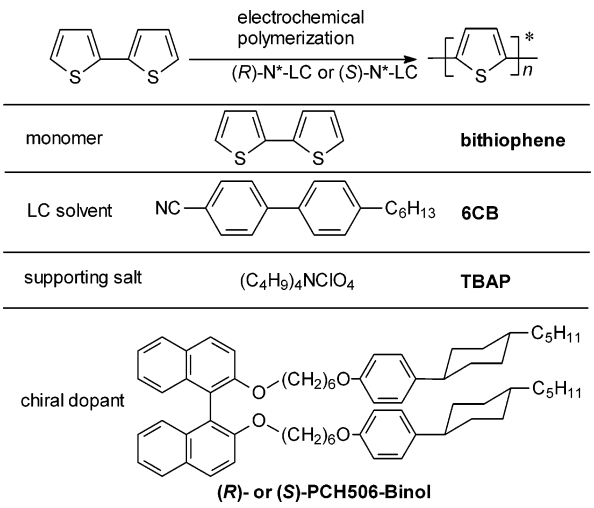

(LC solvent) was prepared as the electrolyte. The N*-LC mixture clearly displayed a chiral nematic LC texture. The solution was heated once to 80 °C to completely dissolve the TBAP, bithiophene, and chiral dopant in the N*-LC solvent. Differential scanning calorimetry (DSC) measurements and polarizing optical microscopy (POM) observations confirmed that both the (*R*)- and (*S*)-N*-LC systems exhibited a thermotropic N*-LC phase. A typical N*-LC fingerprint texture was observed by POM (Figure 1a). The distance between stripes in the texture corresponds to the helical half-pitch.

Polymerization

Figure 2 shows the ionic conductivity of monomer-free (*R*)-N*-LC electrolyte between indium titanium oxide (ITO) glass plates as a function of frequency at 25 °C. The corresponding impedance spectrum has a semicircular section in the Cole−Cole plot at higher frequencies and a linear section at lower frequencies (Figure 2a). On the basis of these results, the monomer-free N*-LC electrolyte can be described by an equivalent electrical circuit as a model of impedance, as shown in Figure 2b. The low ionic dc conductivity ($<10^6$ S/cm) of the LC electrolyte may result in a current-resistance (IR) drop. To compensate for this drop, the electrochemical polymerization was carried out using a two-electrode method with a narrow gap.

The N*-LC mixture was injected between sandwiched ITO electrodes using a Teflon sheet (thickness: 0.19 mm) as a spacer (Figure 3). The reaction cell was heated to 30 °C and then gradually cooled to 12 °C to obtain a good fingerprint texture. A voltage of 4 V was then applied to the cell. The optical texture of the N*-LC mixture remained unchanged upon voltage application. However, repeated voltage scanning by cyclic voltammetry during the polymerization process destroyed the helical structure of the N*-LC, resulting in a transparent mixture. This can be attributed to the unwinding of helicity under the alternating current, where the LC molecules are aligned normal to the substrate (homeotropic alignment). The polymerization temperature was maintained at a constant 12 °C through the use of a custom-made temperature control stage with Peltier element in order to preserve the N*-LC phase. After 30 min, an insoluble and infusible deep blue polymer thin film of ∼29 nm in thickness coated the anode side of the ITO electrode. After washing with methanol, water, acetonitrile, methanol, water, and acetone in order, the polymer film on the ITO was dried under reduced pressure.

The transition temperatures of the N*-LC electrolyte containing the monomer, determined by DSC, were K·10(3)·N*·16(14)·Iso* for the (*R*)-N*-LC electrolyte before polymerization and K·11(3)·N*·16(15)·Iso* after polymerization and K·10(4)·N*·16(15)·Iso* for the (*S*)-N*-LC electrolyte before polymerization and K·11(5)·N*·17(16)·Iso* after polymerization (K, crystal; N*, chiral nematic; Iso*, isotropic). The transition temperatures of the N*-LC solution after electrochemical polymerization were thus slightly higher than before polymerization, suggesting that the monomer in the N*-LC was consumed during polymerization since, in general, impurities in the LC mixture lower the transition temperature. Note that polymerization of thiophene as a monomer using this method did not give a stable film, probably because thiophene has lower polymerization activity than bithiophene in the N*-LC medium.

Electrochemical polymerization of bithiophene was also carried out in N*-LC using (*R*)- or (*S*)- 4-cyano-4′-(1-methylheptyloxy)-biphenyl (CB60*) or (*R*)- or (*S*)-1,1′-bi-2,2′-naphthol (Binol*) as chiral dopants in place of PCH506-Binol. In these cases, however, large amounts of chiral dopant were required to induce formation of the chiral nematic phase compared to the case for PCH506-Binol. This is considered to be due to the lower helical twisting power ($\beta_M < 2$) of CB60* and Binol* compared to PCH506-Binol ($\beta_M = 22.5$). Note that the helical twisting power of the chiral dopant was evaluated from the helical pitch of the N*-LC containing the chiral dopant by the Cano wedge method. The addition of a large amount of the chiral dopant to 6CB caused the transition temperature of the N*-LC to be reduced to less than 0 °C. Polymerization at such low temperature suffered from poor polymerization activity, resulting in a fragile film.

Electrochemical polymerization was also performed using chiral smectic LC composed of the following system.

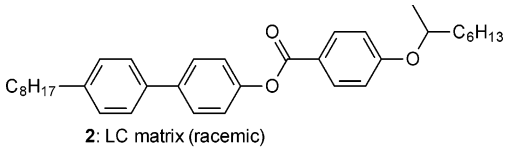

2: LC matrix (racemic)

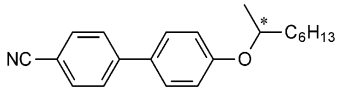

(*R*)- or (*S*)-CB60*: chiral molecule

Although the LC electrolyte containing TBAP and the monomer (LC matrix, 5 mg; CB60*, 5 mg; TBAP, 0.03 mg; bithiophene, 0.1 mg) exhibited a chiral smectic phase, no polymer film could be formed due to the high viscosity of the chiral smectic phase at 7 °C. Deposition was also inhibited by the low conductivity and low mobility of the monomer in the chiral smectic matrix. These results imply that electrochemical polymerization in thermotropic LC requires both a chiral dopant with sufficient helical twisting power to form N*-LC and an N*-LC matrix of sufficiently low viscosity to transport ions and monomers easily.

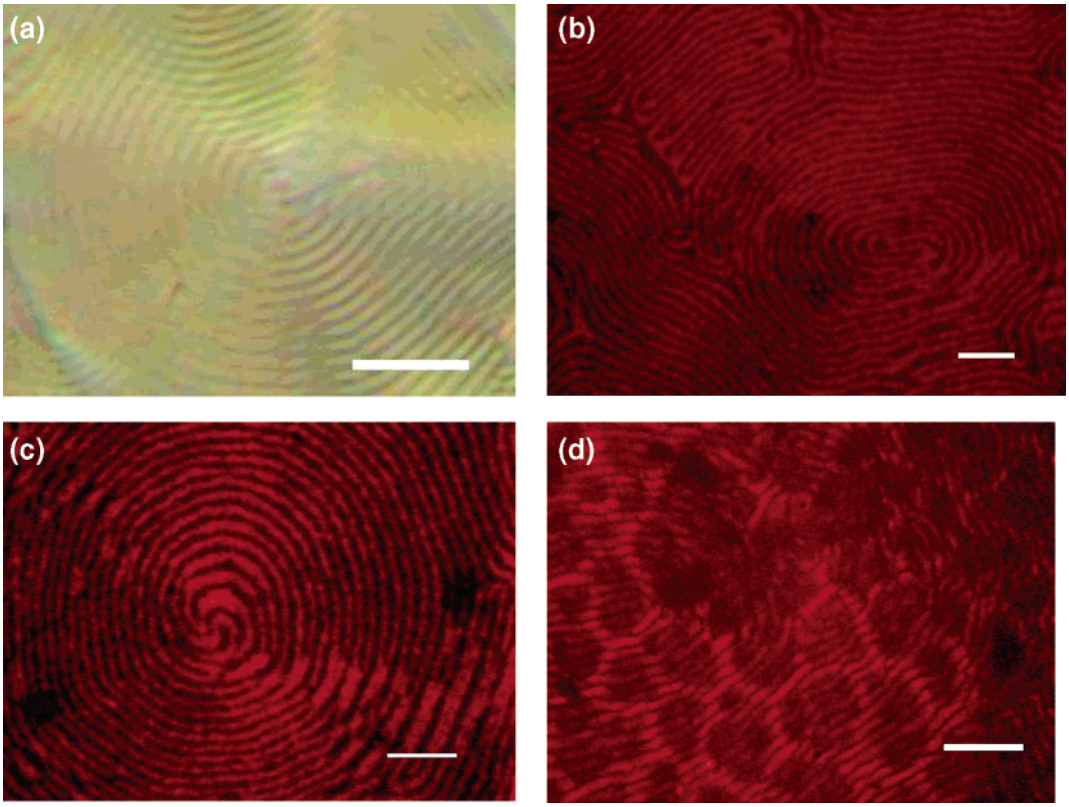

Figure 1. (a) Polarizing optical micrograph of (*R*)-PCH506-Binol electrolyte at 10 °C. (b−d) Phase-contrast optical micrographs (no polarizer) showing three areas of a (*R*)-PBTh* film at 25 °C (scale bar: 10 μm): (b) fingerprint texture, (c) double spiral texture, (d) fingerprint texture on polygonal texture.

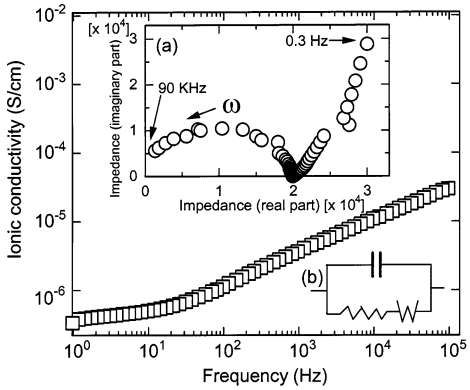

Figure 2. Ionic conductivity as a function of frequency. (a) Cole−Cole plots for the electrolyte. (b) Equivalent electrical circuit used to model the impedance.

Characterization

Optical Texture. Phase-contrast optical microscopy (PCM) of the polybithiophene prepared in (*R*)-N*-LC [(*R*)-PBTh*] (Figure 1b,c) revealed the spiral texture of the polymer, resembling that of the original N*-LC system. Figure 1d shows another part of the same (*R*)-PBTh* film. This image implies that the sample consists of multiple layers and also reveals some overlap between the spiral texture (upper layer) and the polygonal network structure (lower layer) due to changes in the LC anchoring condition. This unique pattern mimics the N*-LC texture during electrochemical polymerization. Thus, the present electrochemical polymerization method also provides detailed information regarding the classification of the LC structure.

The PBTh* film exhibited no birefringence under POM, suggesting that the texture is not due to the LC but due to the polymer itself. The PBTh* thus synthesized appears to replicate the structure of the N*-LC, demonstrating that the N*-LC is effective as an asymmetric reaction field.

Cyclic Voltammetry. Figure 4 shows the results of cyclic voltammetry measurements of (*R*)-PBTh* films (vs Ag/Ag^+) at various scan rates in 0.1 M TBAP/acetonitrile solution. The redox switching in monomer-free electrolyte solution indicates a well-defined and quasi-reversible redox process. The polymers prepared in both (*R*)- and (*S*)-chiral electrolyte exhibited the same redox behavior, suggesting that the polymers have basically the same structure. Both are electroactive and were well adhered to the ITO electrode.

Optical Properties. Circular dichroism (CD) spectra of the polymers are shown in Figure 5.[21] Both the (*R*)- and (*S*)-PBTh* films exhibited strong mirror-image bisignate Cotton effects in the $\pi-\pi^*$ transition region of the polymer main chain in the reduced state. This means that (*R*)- and (*S*)-PBTh* have the same degree of chirality but opposite sense. In the oxidized state, the CD spectra of the polymers showed a decrease in intensity and an inversion in the sign of the Cotton effect. The mirror-image relationship between (*R*)- and (*S*)-PBTh* cannot due to the chiral dopant employed in polymerization because the Cotton effect of the chiral dopant is only observed at shorter wavelengths between 240 and 340 nm, as shown in Figure 6. The phenomenon of reversible inversion of the sign of the Cotton effect at 592 nm in redox processes, via a change in the electronic state of the polymer, indicates that the polymers have an inherently chiral structure.

Figure 7 shows the ultraviolet and visible (UV−vis) absorption spectra and CD spectra of (*R*)-PBTh* at various voltages vs Ag/Ag^+ in monomer-free 0.1 M

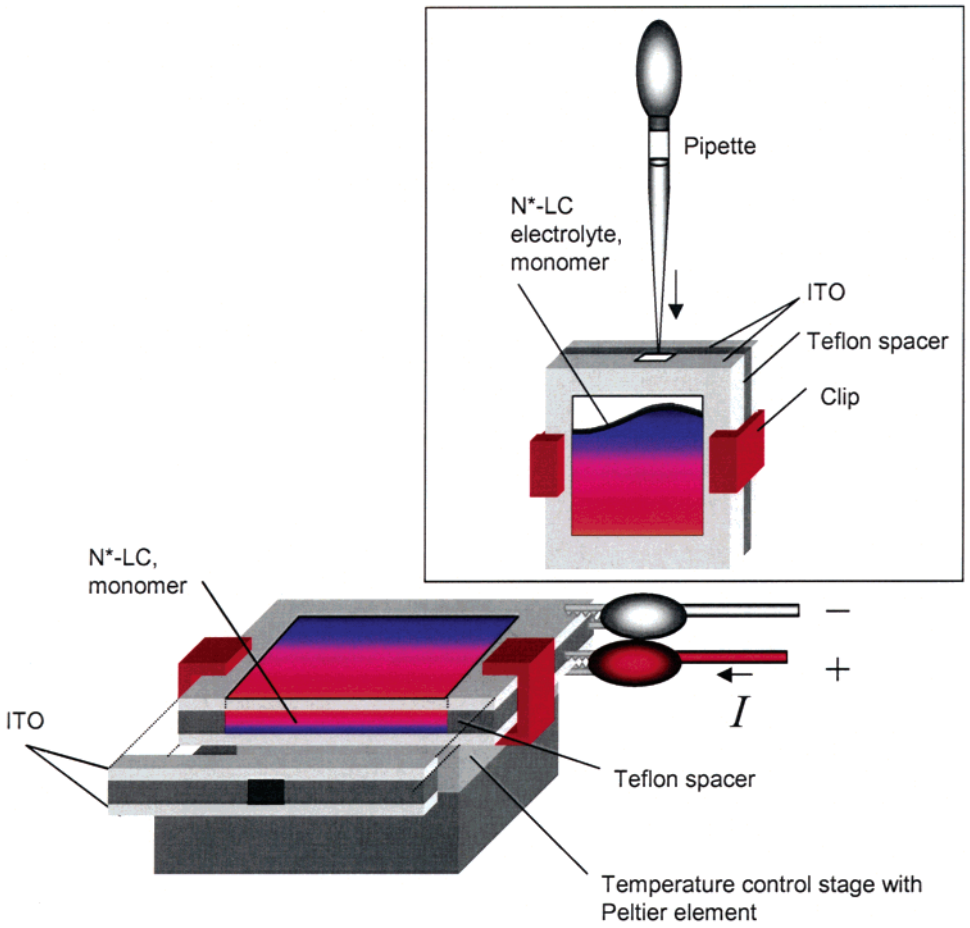

Figure 3. Polymerization cell.

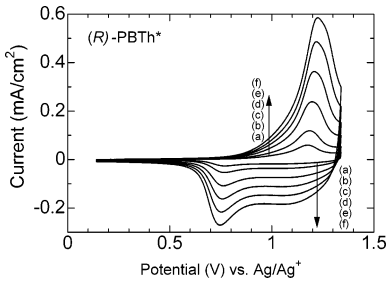

Figure 4. Cyclic voltammetry (vs Ag/Ag^+) of (*R*)-PBTh* thin film deposited on ITO glass in monomer-free solution of 0.1 M TBAP/acetonitrile at scan rates of (a) 10 (b) 20, (c) 40, (d) 60, (e) 80 and (f) 100 mV s^{-1}.

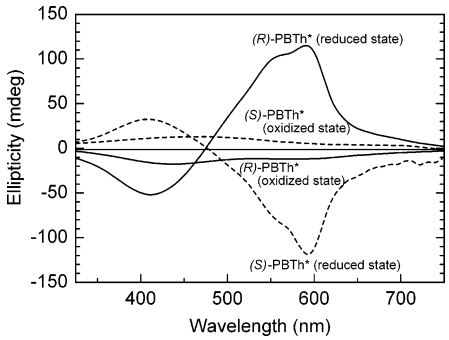

Figure 5. (*R*)- and (*S*)-PBTh* films in oxidized and reduced states. The oxidized and reduced states of the polymer were produced by applications of potential (+1.3 V: oxidized state; 0.1 V: reduced state vs Ag/Ag^+) in 0.1 M TBAP/acetonitrile solution.

TBAP/acetonitrile solution. Upon oxidation, the peak at 492 nm in the absorption spectrum associated with the $\pi-\pi^*$ transition of the polymer main chain becomes weaker, while the peak at 680 nm (1.8 eV, mid-gap) due to generation of radical cations on the polymer main chain becomes stronger. The color of the polymer also changes from red to dark blue (Figure 8) upon oxidation, accompanied by the emergence of a broad absorption band in the NIR region (Figure 9). This transition is also marked by a weakening of the positive extremum at 592 nm and the negative extremum at 410 nm in the CD spectrum and the appearance of an isosbestic point at 461 nm. Application of 0.83 or 0.15 V as a reduction process leads to restoration of these peaks to the original intensity in the reduced state in both the UV−vis and CD spectra (Figure 7). This result indicates that the polythiophene main chain itself is a chiral structure and that the Cotton effect of the polymer can be changed by adjusting the conditions of electrochemical polymerization. However, the redox process did not induce any change in the optical texture or surface structure of PBTh*s. The large change in the Cotton effect of the polymer by redox reaction in TBAP/acetonitrile solution is attributable to the weaker Cotton effect of the oxidized state. This electrochemical process allows the CD intensity to be controlled.

The CD spectra of the polymer in poor solvents or of the film of polythiophene cast with an optically active substituent have been interpreted as being due to exciton coupling, usually with a Davydov splitting of the same order as the vibronic splitting.[22] Exciton coupling requires the presence of an unconjugated chromophore

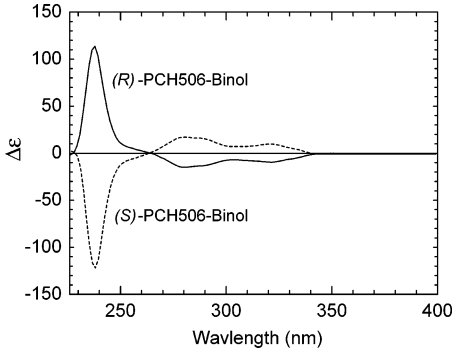

Figure 6. CD spectra of (*R*)- and (*S*)-PCH506-Binol in THF.

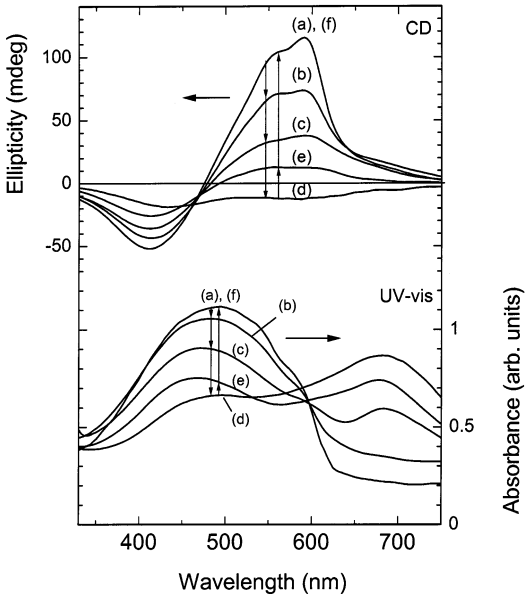

Figure 7. In-situ CD spectra (top) and UV−vis absorption spectra (bottom) of (*R*)-PBTh* on an ITO electrode at various potentials vs Ag/Ag^+ reference in a monomer-free 0.1 M TBAP/acetonitrile solution: (a) 0.20, (b) 0.91, (c) 1.07, (d) 1.30, (e) 0.83, and (f) 0.15 V.

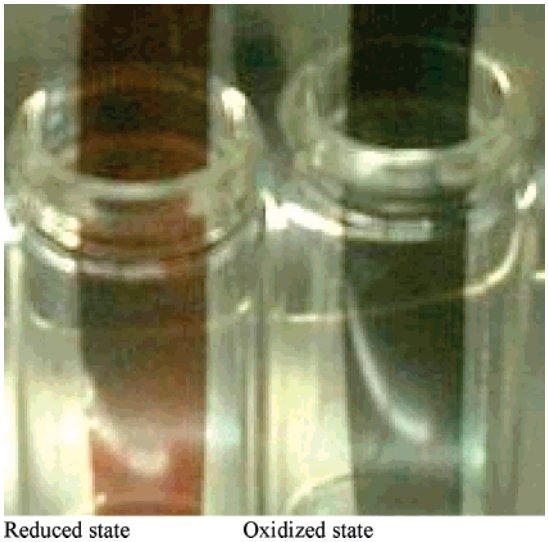

Figure 8. Photographs of polymer on ITO glass in reduced and oxidized state.

in the chiral arrangement, which can occur through intrachain and interchain interaction in the aggregate state.[23−25] The CD spectra of reduced PBTh* reveals a

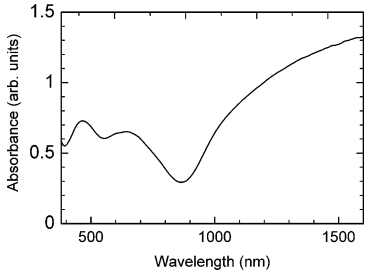

Figure 9. UV−vis−NIR spectrum of (*R*)-PBTh* in the oxidized state.

bisignate Cotton effect, while that in the oxidized state does not.

The observation of such a bisignate band for PBTh* may suggest the presence of an intermolecular process upon aggregate formation.[26] In this case, the aggregate-induced band is a charge transfer-type $\pi-\pi^*$ stacking of the polymer backbone, arising due to electronic communication.[27] Alternatively, the conjugated polymer main chain may be helically twisted, thereby producing a chiral chromophore. In the helical aggregation state of the polymer, several hierarchical levels of helical structure, from molecular to macroscopic, are possible. This redox-induced change in CD for PBTh* can therefore be reasonably explained as being due to the intercalation of the perchlorate ion and solvent between polymer main chains at the molecular level, resulting in extension of the distance between polymer main chains in the oxidized state. In the reduced state, (*R*)-PBTh* shows a positive first Cotton effect at longer wavelength and negative second cotton effect, and (*S*)-PBTh* shows a negative first Cotton effect and positive second Cotton effect. In this case, the exciton-coupled bisignate couplet in the CD spectra indicates a one-handed helical assembly, with a positive couplet (chirality of the transition moment is clockwise) for (*R*)-PTBh* and a negative couplet (chirality of the transition moment is counter clockwise) for (*S*)-PTBh*. In the oxidized state, the polymers exhibit no such bisignate character, and the sign of the Cotton effect at around 600 nm is the opposite to that in the reduced state. This result implies that the helical aggregation is released upon doping, losing the chiral aggregation structure. However, the polymers still exhibit a Cotton effect originating from the chiral structure of the polymer main chain.

Another explanation is possible for this phenomenon. It has been reported that a solid film of polythiophene derivatives exhibits conformational-induced chromism through a doping−dedoping redox process.[28] This optical effect was found to be reversible and could not be attributed to any degradation of the polymer. Such optical effects are considered to be related to a reversible transition between the coplanar form of the highly conjugated state and the nonplanar form of the less-conjugated structure of the polymer main chain.[29] The electrochromism of PBTh*s in CD during the redox process may therefore originate from small changes in the dihedral angle between neighboring thiophene unit cells.

In the case of helical polyacetylene, the dihedral angle ranges from 0.02° to 0.23°, and the polymer displays a strong Cotton effect in the CD spectrum. The small sequential change in torsion angle in the one-handed twist direction between neighboring units of the polyacetylene results in a consistent Cotton effect. It is

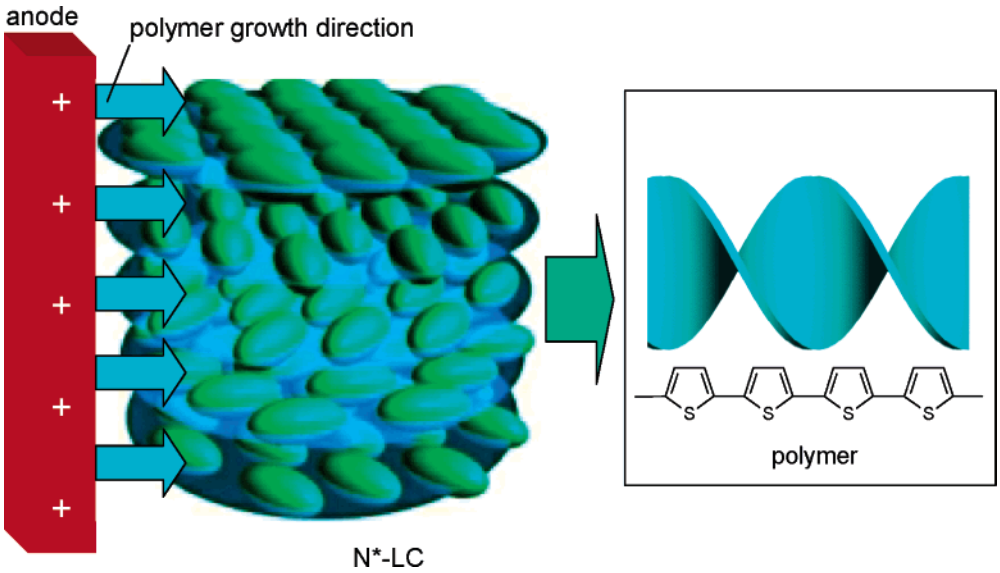

Figure 10. Polymerization mechanism for PBTh* in N*-LC field.

possible that the change in the Cotton effect of PBTh* in the film state is caused by small dihedral angle changes as a result of the alternating potential during the repeated redox doping−dedoping process. This process generates polaron and bipolaron states in the polymer. In the monomer unit, although the dihedral angle must be very small, the small sequential change in torsion angle in the one direction along the polymer main chain as virtual chiral axis is considered to result in strong chirality for PBTh*, representing a "polymer effect" in chiral chemistry. This may be closely related to the elastic behavior of the polymer during the redox process, which would allow structural restoration between the doping and dedoping state in the film. The phenomenon of reversible change in the Cotton effect can therefore be regarded as a form of "electrochemical isomerization".

The PBTh* structure must be reflected in both the molecular form and the N*-LC aggregation state. The CD bands thus result from both intermolecular aggregation of the chromophore and helical twisting of the polymer main chain.

Electrochemical polymerization of bithiophene in the LC mixture using the isotropic phase (30 °C) resulted in a polymer that did not have a spiral structure. As seen from the SEM photograph, the resultant PBTh had a random globular structure, with no Cotton effect. Similarly, no Cotton effect was exhibited by a polymer synthesized by electrochemical polymerization using nematic liquid crystal (N-LC) without a chiral dopant under the same polymerization conditions as for N*-LC. These results suggest that the chiral nematic LC environment is essential for synthesis of chiral bithiophene. Thus, electrochemical polymerization in an N*-LC field allows for the preparation of electrically and optically active, solid-state conjugated polymers with controllable Cotton effect.

Polymerization Model in N*-LC Field

The PBTh* film exhibited chiroptical properties and formed a chiral structure similar to that of the N*-LC. The structure formed during polymerization was preserved even after washing. None of the chiral molecules reacted chemically with the monomer during polymerization, demonstrating that the electrolyte behaves as a matrix only.[18] The insolubility and infusibility of PBTh* are essential for preservation of the metastable chiral structure. Figure 10 shows a plausible polymerization mechanism for PBTh* in a N*-LC field. In this model, the polymer grows from the anode to the cathode through the three-dimensional helical structure of the N*-LC. The polymer main chain grows with a twist in only one sense during the polymerization process, forming a bundle structure through the aggregation of twisted polymer chains by van der Waals forces. The bundle forms a macroscopic cholesteric fingerlike structure. It should be emphasized that the polymerization mechanism in an N*-LC field differs from that for an achiral monomer using a chiral catalyst.

Repeating Redox Properties and CD

The large changes in both color and Cotton effect through the electrochemical doping−dedoping process suggest that PBTh* can be used as an electrochromic material. The electrochromic switching behavior of PBTh* was examined through observation of changes in the absorption and CD spectra upon repeated changes in the applied voltage between the reduced and oxidized states. A platinum plate was used as the counter electrode, and the sample of (*R*)- or (*S*)-PBTh* film was prepared by deposition on an ITO-coated glass by electrochemical polymerization in N*-LC. Figure 11 shows the absorption changes in (*R*)-PBTh* with a repeating voltage scanning between 0.1 and 1.3 V vs Ag/Ag^+ in 0.1 M TBAP/acetonitrile electrolyte (100 mV s^{-1}). The absorption intensities were monitored at 492 and 680 nm at 12 s intervals. In the oxidization process (1.3 V vs Ag/Ag^+), the absorption intensity at 492 nm weakened, while that at 680 nm became stronger. This change in absorption intensity was found to be repeatable upon subsequent reduction. As shown in Figure 12, the CD intensities of (*R*)- and (*S*)-PBTh* during voltage scanning also underwent a reversible, symmetrical change. The CD intensities at 592 nm were lowest at 1.3 V vs Ag/Ag^+ (oxidized state), and both polymers exhibited Cotton effects: negative for (*R*)-PBTh* and positive for (*S*)-PBTh*. The application of 0.1 V vs Ag/Ag^+, giving the reduced state, leads to a subsequent

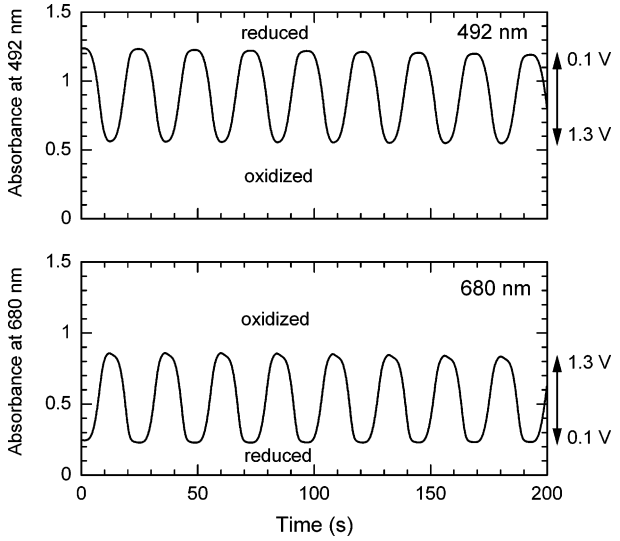

Figure 11. Reversible change in UV−vis absorption intensities at 492 nm (upper) and 680 nm (lower) for an electrochromic cell based on (*R*)-PBTh* at voltages of 0.1−1.3 V vs Ag/Ag^+ (scan rate: 100 mV s^{-1}).

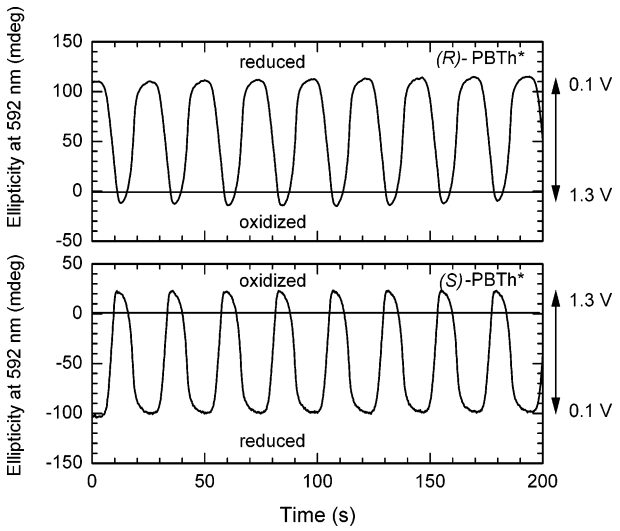

Figure 12. Reversible change in CD intensity at 592 nm for a chiral electrochromic cell based on (*R*)-PBTh* (upper) and (*S*)-PBTh* (lower) at voltages of 0.1−1.3 V vs Ag/Ag^+ (scan rate: 100 mV s^{-1}).

increase in CD intensity at 592 nm, with opposite sign of Cotton effect with respect to the oxidized state. Thus, control of the redox process allows for a reversible change in CD intensity.

Conclusion

PBTh was demonstrated to replicate the spiral morphology of N*-LC used as a solvent in electrochemical polymerization, affording an optically active conjugated polymer (PBTh*) exhibiting optically active electrochromism. This method allows active control of the optical activity of the polymer. The proposed synthesis method provides new possibilities for chiral engineering, allowing for the synthesis of a range of conjugated polymers with chiroptical properties and extending the applications of such polymers in bioscience and engineering. This study also highlights the importance and versatility of chiral reaction fields for chemical synthesis.

Experimental Section

Optical Measurements. Optical absorption spectra were measured at room temperature using a HITACHI U-2000 spectrometer with a quartz cell. Circular dichroism (CD) spectra were obtained by JASCO J-720. Infrared spectroscopic measurements were carried out using a Jasco 550 Fourier infrared (FT-IR) spectrometer. Differential scanning calorimetry (DSC) was performed using a TA instruments Q100 DSC instrument at a rate of 10 °C/min under a N_2 gas flow. Optical textures were observed by polarizing optical microscopy (POM) using a Nikon ECLIPS E 400 POL polarizing microscope equipped with a Linkam TM 600PM heating-and-cooling stage. Temperature control during polymerization was achieved using a custom-made cooling stage based on a Peltier element. Optical phase-contrast microscopy (PCM) observations of the polymer were carried out using a WRAYMER BX-3500T microscope equipped with a phase contrast optical unit. Scanning electron microscopy (SEM) observations were carried out using a JEOL ED electron microscope. Electrochemical measurements of polymers were obtained using an ALS660A electrochemical analyzer (BAS). Film thickness measurements were performed using a ZYGO new view5032 3-D surface structure analysis microscope with frequency domain analysis method.

Materials. The chiral dopants, (*R*)- or (*S*)-1,1′-binaphthyl-2,2′-bis[*p*-(*trans*-4-pentylcyclohexyl)phenoxy-1-hexyl] ether [abbreviated (*R*)- or (*S*)-PCH506−Binol], used for this study were prepared by a Williamson etherification reaction of chiroptical (*R*)-(+)- and (*S*)-(−)-1,1′-2-binaphthols with phenylcyclohexyl derivatives, respectively, as described in the literature.[11] However, in this experiment, we carried out the synthesis by using 18-crown-6-ether as a phase transfer catalyst in acetone at 60 °C, instead of using potassium iodide in cyclohexanone at 156 °C, to avoid partial racemization during the etherification reaction. 1-[*p*-(*trans*-4-*n*-Pentylcyclohexyl)phenoxy]-6-bromohexane was synthesized by the method described in the literature.[31] The chemical structure of the chiral dopants was confirmed with NMR. 4-Cyano-4′-*n*-hexyl biphenyl (6CB) was purchased from Merck Ltd. Bithiophene (BTh) was obtained from Sigma Aldrich and was purified by recrystallization from ethanol prior to use. The indium tin oxide (ITO) glass consists of a 0.2−0.3 μm thick ITO layer on glass (9 Ω/cm^2).

(*R*)-(+)-1,1′-Binaphthyl-2,2′-bis[*p*-(*trans*-4-pentylcyclohexyl)phenoxy-1-hexyl] Ether [(*R*)-PCH506-Binol]. A solution of (*R*)-(+)-1,1′-bi-2-naphthol (1 g, 3.5 mmol), 1-[*p*-(*trans*-4-*n*-pentylcyclohexyl)phenoxy]-6-bromohexane (3.1 g, 7.3 mmol), K_2CO_3 (1.4 g, 10 mmol), and 18-crown-6-ether (46 mg, 0.2 mmol) in acetone (100 mL) was refluxed at 60 °C. After 24 h, the solution was evaporated, thoroughly washed with water, and extracted with ether. The organic layer was evaporated. Crude product was purified by column chromatography (silica gel, $CHCl_3$/*n*-hexane = 1) to afford 2.7 g of white solid (yield = 82%). Anal. Calcd for $C_{68}H_{92}O_4$: C, 83.90; H, 9.53. Found: C, 84.02; H, 9.22. IR (KBr, cm^{-1}): 2937, 2884, 1515, 1235 (COC st). ^{1}H NMR (500 MHz, $CDCl_3$, ppm): 0.87−1.87 (m, 33H, CH, CH_2, CH_3), 2.35 2.45 (m, 1H, ph), 3.71 (t, J = 6.8 Hz, 2H, CH_2O), 3.9−4.0 (m, 2H, CH_2O), 6.8−7.9 (m, 8H, ph). ^{13}C NMR (125 MHz, $CDCl_3$, ppm): 14.1, 22.7, 25.4, 25.5, 26.6, 29.0, 29.3, 32.2, 33.6, 34.6, 37.3, 37.4, 43.7, 67.6, 69.6, 114.0, 115.7, 120.6, 123.2, 125.2, 125.8, 127.3, 127.5, 128.8, 129.0, 133.9, 139.6, 154.2, 156.9. $[\alpha]^{23}_D$ = +22.5 ° (THF).

(*S*)-(−)-1,1′-Binaphthyl-2,2′-bis[*p*-(*trans*-4-pentylcyclohexyl)phenoxy-1-hexyl] Ether [(*S*)-PCH506-Binol]. This compound was prepared using a method similar to that described for (*R*)-PCH506-Binol). Quantity used: PCH506Br (4.4 g, 10.5 mmol), K_2CO_3 (1.4 g, 10.5 mmol), 18-crown-6 ether (46 mg, 0.2 mmol), and acetone (100 mL). Yield: 57%, 1.9 g (white crystal). Anal. Calcd for $C_{68}H_{92}O_4$: C, 83.90; H, 9.53; O, 6.57. Found: C, 83.92; H, 9.19. IR (KBr, cm^{-1}): 2940, 2843, 1514, 1247 (COC st). ^{1}H NMR (500 MHz, $CDCl_3$, ppm): 0.87−1.87 (m, 33H, CH, CH_2, CH_3), 2.35−2.45 (m, 1H, ph), 3.72 (t, J = 6.8 Hz, 2H, CH_2O), 3.86−3.98 (m, 2H, CH_2O), 6.76−7.90 (m, 8H, ph).

^{13}C NMR (125 MHz, $CDCl_3$, ppm): 14.1 (CH, CH_2, CH_3), 22.7, 25.4, 25.4, 26.6, 29.0, 29.3, 32.2, 33.6, 34.6, 37.3, 37.4, 43.7, 67.6, 69.6, 114.0, 115.7, 120.6, 123.2, 125.2, 125.8, 127.3, 127.5, 128.8, 129.0, 133.9, 139.6, 154.2, 156.9. $[\alpha]^{23}_D = -23.3°$ (THF).

Acknowledgment. This work was supported by Grant-in-Aids for Scientific Research from the Ministry of Education, Culture, Sports and Science Technology, Japan. We thank Dr. S. Iimura and T. Asano (Ibaraki Prefectural Government Industrial Technology Institute) for film thickness measurements.

References and Notes

(1) Langeveld-Voss, B. N. W.; Janssen, R. A. J.; Meijer, E. W. *J. Mol. Struct.* **2000**, *521*, 285.
(2) Emiel. P.; Delmotte, A.; Janssen, R. A. J.; Meijer, E. W. *Adv. Mater.* **1997**, *9*, 493.
(3) Osaka, I.; Nakamura, A.; Inoue, Y.; Akagi, K. *Trans. Mater. Res. Soc. Jpn.* **2002**, *27*, 567.
(4) Goto, H.; Akagi, K. *Synth. Met.* **2001**, *119*, 165.
(5) Moore, J. S.; Gorman, C. B.; Grubbs, R. H. *J. Am. Chem. Soc.* **1991**, *113*, 1704.
(6) Tang, H.; Fujiki, M.; Sato, T. *Macromolecule*s **2002**, *35*, 6439.
(7) Nakao, H.; Mayahara, Y.; Nomura, R.; Tabata, M.; Masuda, T. *Macromolecules* **2000**, *33*, 3978.
(8) Tsuruta, T.; Inoue, S.; Furukawa, *J. Macromol. Chem.* **1965**, *84*, 298.
(9) Ebert, P. E.; Price, C. *J. Polym. Sci.* **1959**, *34*, 157.
(10) Yashima, E.; Maeda, K. Okamoto, Y. *Nature (London)* **1999**, *399*, 449.
(11) Akagi, K.; Piao, G.; Kaneko, S.; Sakamaki, K.; Shirakawa, H.; Kyotani, M. *Science* **1998**, *282*, 1683.
(12) Shirakawa, H. *Curr. Appl. Phys.* **2001**, *1*, 88.
(13) Sonmez, G.; Scottland, P.; Zong, K.; Reynolds, J. R. *J. Mater. Chem.* **2001**, *11*, 289.
(14) (a) Schwendeman, I.; Hwang, J.; Welsh, D.; Tarner, D. B.; Reynolds, J. R. *Adv. Mater.* **2001**, *13*, 634. (b) Zong, K.; Abboud, K. A.; Reynolds, J. R. *Tetrahedron Lett.* **2004**, *45*, 4973. (c) DuBois, C. J.; Abboud, K. A.; Reynolds, J. R. *J. Phys. Chem. B* **2004**, *108*, 8550. (d) Tsuie, B.; Reddinger, J.; Soting, G.; Soloducho, J.; Katrizky, A.; Reynolds, J. R. *J. Mater. Chem.* **1999**, *9*, 2189. (e) Groenendaal, B.; Jonas, F.; Freitag, D.; Pielartzik, H.; Reynolds, J. R. *Adv. Mater.* **2000**, *12*, 481. (f) Gaupp, C. L.; Welsh, D.; Reynolds, J. R. *Macromol. Rapid Commun.* **2002**, *23*, 885.
(15) Granstöm, M.; Berggern, M.; Inganäs, O. *Science* **1995**, *267*, 1479.
(16) Burroughes, J. H.; Bradley, D. D. C.; Brown, A. R.; Marks, R. N.; Mackay, K.; Friend, R. H.; Burns, P. L.; Holmes, A. B. *Nature (London)* **1990**, *347*, 539.
(17) Kingsborough, R. P.; Swager, T. M. *Adv. Mater.* **1998**, *10*, 541.
(18) Goto, H.; Akagi, K. *Macromol. Rapid Commun.* **2004**, *25*, 1482.
(19) Solladié, G.; Zimmermann, G. *Angew. Chem. Int. Ed. Engl.* **1984**, *23*, 348.
(20) Huck, N. P. M.; Jaeger, W. F.; Lange, B.; Fringe, B. L. *Science* **1996**, *273*, 1686.
(21) CD measurements were carried out by rotating the sample to exclude both the artifact and linear polarization in Cotton effect.
(22) Iarossi, D.; Mucci, A.; Parenti, F.; Schenetti, L.; Seeber, R.; Zanardi, C.; Forni, A.; Tonelli, M. *Chem.—Eur. J.* **2001**, *7*, 676.
(23) Langeveld-Voss, N. W. B.; Janssen, R. A. J.; Christiaans, M. P. T.; Meskers, S. C. J.; Dekkers, H. P. J. M.; Meijer, E. W. *J. Am. Chem. Soc.* **1996**, *118*, 4908.
(24) Andereaniu, F.; Angiolini, L.; Caretta, D.; Salatelli, E. *J. Mater. Chem.* **1998**, *8*, 1109.
(25) Berova, N.; Gargiulo, D.; Derguini, F.; Nakanishi, K.; Harada, N. *J. Am. Chem. Soc.* **1993**, *115*, 4769.
(26) Steffen, W.; Köhler, B.; Altmann, M.; Scherf, U.; Stizer, K.; zur Loye, H.-C.; Bunz, U. H. F. *Chem.—Eur. J.* **2001**, 7, 117.
(27) Miteva, T.; Palmer, L.; Kloppenburg, L.; Neher, D.; Bunz, U. H. F. *Macromolecules* **2000**, *33*, 652.
(28) Patil, A. O.; Heeger, A. J.; Wudl, F. *Chem. Rev.* **1988**, *88*, 183.
(29) Leclerc, M.; Fäid, K. In *Handbook of Conducting Polymers,* 2nd ed.; Skotheim, T. A., Elsenbaumer, R. L., Reynolds, J. R., Eds.; Marcel Dekker: New York, 1998; p 695.
(30) Goto, H.; Akagi, K. Jpn Patent 362979, 2002; *Chem. Abstr.* **2003**, *139*, 344169.
(31) Kiebooms, R. H. L.; Goto, H.; Akagi, K. *Macromolecules* **2001**, *34*, 7989.

MA048505N